PHYSICAL REVIEW B VOLUME 50, NUMBER 1 1 JULY 1994-I

Conserving approximations for the attractive Holstein and Hubbard models

J. K. Freericks
Department of Physics, University of California, Davis, California 95616
(Received 27 January 1994)

Conserving approximations are applied to the attractive Holstein and Hubbard models (on an infinite-dimensional hypercubic lattice). All effects of nonconstant density of states and vertex corrections are taken into account in the weak-coupling regime. Infinite summation of certain classes of diagrams turns out to be a quantitatively less accurate approximation than truncation of the conserving approximations to a finite order, but the infinite summation approximations do show the correct qualitative behavior of generating a peak in the transition temperature as the interaction strength increases.

I. INTRODUCTION

It is generally believed that the theoretical aspects of conventional superconductors are well understood and that quantitative predictions agree with experiment.[1,2] The reason why low-temperature superconductors can be described accurately for all physical values of the electron-phonon coupling is due to Migdal's theorem:[3] the ratio of the electron mass to the ion-core mass provides the small parameter that guarantees rapid convergence of the theory. Eliashberg[4] generalized Migdal's theorem to the superconducting state and provided the framework for quantitative calculations of the superconducting properties of real materials.[1,2]

A more precise way of stating Migdal's theorem is to say that only the electrons that lie in an energy shell of width $\Omega_{\rm Debye}$ about the Fermi surface are affected by phonon scattering, and the only important scattering events involve the virtual emission and reabsorption of phonons in an *ordered* fashion, where the last emitted phonon is the first absorbed phonon, and so on. Migdal-Eliashberg (ME) theory neglects vertex corrections (which involve crossings of the phonon lines) and is an accurate approximation for small phonon frequencies. The remaining unanswered question is how large does the phonon frequency have to be before the effects of vertex corrections are observable?

There are many materials that are hypothesized to be electron-phonon-mediated superconductors, but have large phonon frequencies. $Ba_{1-x}K_xBiO_3$ is a charge-density-wave (CDW) insulator at zero doping ($x = 0$), but becomes a superconductor (SC) away from half filling[5] ($x \geq 0.37$). The maximum phonon frequency is $\Omega_{\rm max} = 80$ meV for the optical oxygen modes,[6] while the bandwidth[7] is $W = 4$ eV, so the ratio of the phonon energy scale to the electronic energy scale is $\Omega_{\rm max}/W = 0.02$. Are vertex corrections important for this material?

Alkali-metal-doped C_{60} is another superconducting material that is hypothesized to have an electron-phonon pairing mechanism. There are very high-frequency phonons that correspond to distorting the C_{60} cage[8] ($\Omega \approx 0.2$ eV), while the electronic bandwidth is quite narrow[9] ($W = 1.0$ eV), resulting in $\Omega_{\rm max}/W \approx 0.2$. Clearly, vertex corrections must play an important role in phonon-mediated pairing mechanisms in these materials.

The effect of vertex corrections on superconducting properties, in particular, on the superconducting transition temperature, has been studied in the past.[10–12] Grabowski and Sham[10] showed that vertex corrections lower T_c for the repulsive electron gas, with $T_c \to 0$ for some critical value of the plasma frequency. The electron-phonon interaction has also been examined,[11,12] and, in general, vertex corrections also cause T_c to drop. Is this always the effect of vertex corrections, or can vertex corrections sometimes cause an enhancement to T_c?

In this contribution the effects of vertex corrections are examined in a systematic fashion via weak-coupling conserving approximations for the attractive Holstein[13] and Hubbard[14] models. The effects of Coulomb repulsion are explicitly neglected here. A detailed comparison of these perturbation schemes can be made to exact results for these models in the infinite-dimensional limit to determine which weak-coupling approximation is the most accurate.

The Holstein model consists of conduction electrons that interact with localized (Einstein) phonons:

$$H = -\frac{t^*}{2\sqrt{d}} \sum_{\langle j,k\rangle\sigma} (c^\dagger_{j\sigma} c_{k\sigma} + c^\dagger_{k\sigma} c_{j\sigma}) + \sum_j (g x_j - \mu)(n_{j\uparrow} + n_{j\downarrow} - 1) + \frac{1}{2} M\Omega^2 \sum_j x_j^2 + \frac{1}{2} \sum_j \frac{p_j^2}{M}, \quad (1)$$

where $c^\dagger_{j\sigma}$ ($c_{j\sigma}$) creates (destroys) an electron at site j with spin σ, $n_{j\sigma} = c^\dagger_{j\sigma} c_{j\sigma}$ is the electron number operator, and x_j (p_j) is the phonon coordinate (momentum) at site j. The hopping matrix elements connect the nearest neighbors of a hypercubic lattice in d dimensions. The unit of energy is chosen to be the rescaled

matrix element t^*. The phonon has a mass M (chosen to be $M = 1$), a frequency Ω, and a spring constant $\kappa \equiv M\Omega^2$ associated with it. The electron-phonon coupling constant (deformation potential) is denoted by g; the effective electron-electron interaction strength is then the bipolaron binding energy

$$U \equiv -\frac{g^2}{M\Omega^2} = -\frac{g^2}{\kappa} . \tag{2}$$

The chemical potential is denoted by μ and particle-hole symmetry occurs for $\mu = 0$.

In the instantaneous limit where U remains finite and g and Ω are large compared to the bandwidth ($g, \Omega \to \infty, U =$ finite), the Holstein model maps onto the attractive Hubbard model[14]

$$H = -\frac{t^*}{2\sqrt{d}} \sum_{\langle j,k\rangle\sigma} (c^\dagger_{j\sigma} c_{k\sigma} + c^\dagger_{k\sigma} c_{j\sigma}) - \mu \sum_j (n_{j\uparrow} + n_{j\downarrow})$$
$$+ U \sum_j (n_{j\uparrow} - \tfrac{1}{2})(n_{j\downarrow} - \tfrac{1}{2}) \tag{3}$$

with U defined by Eq. (2).

The weak-coupling theory is based upon the conserving approximations of Baym and Kadanoff:[15] the free energy functional Φ is approximated by a series expansion of skeleton diagrams of the dressed Green's function G; the self-energy $\Sigma(i\omega_n)$ is determined by functional differentiation $\Sigma(i\omega_n) = \delta\Phi/\delta G(i\omega_n)$ at each Matsubara frequency $\omega_n \equiv (2n+1)\pi T$; and the irreducible vertex functions $\Gamma(i\omega_m, i\omega_n)$ (in the relevant channels) are determined by a second functional differentiation.

Independently, van Dongen[16] and Martín-Rodero and Flores[17] showed that the free energy must be expanded to order U^2 to determine the correct transition temperature in the limit $|U| \to 0$ for the Hubbard model at half filling. The vertex corrections reduced the Hartree-Fock transition temperature by a factor of order 3, but the gap ratio $2\Delta(0)/k_B T_c \approx 3.53$ was unchanged (to lowest order).

In addition to reproducing the weak-coupling limit properly, one hopes that the conserving approximations will also be able to reproduce the peak in the transition temperature as a function of interaction strength that occurs as the system crosses over from a weak-coupling regime (where pair formation and condensation both occur at T_c) to a strong-coupling regime (where preformed pairs order at a lower temperature).[18,19] It will turn out that this feature is not easily reproduced by a truncated conserving approximation.

The infinite-dimensional limit of Metzner and Vollhardt[20] is taken ($d \to \infty$), in which the electronic many-body problem becomes a local (impurity) problem that retains its complicated dynamics in time. The large-dimensional limit is quite useful because both the Holstein[21] and Hubbard[22–24] models can be solved exactly using the quantum Monte Carlo (QMC) techniques of Hirsch and Fye.[25] These exact solutions have many of the qualitative features of the many-body problem in finite dimensions. They also provide a unique testing ground for various weak-coupling theories, since the approximate theory can be compared directly to the exact solution in the thermodynamic limit.

In the infinite-dimensional limit, the hopping integral is scaled to zero in such a fashion that the free-electron kinetic energy remains finite while the self-energy for the single-particle Green's function and the irreducible vertex functions have no momentum dependence and are functionals of the local Green's function.[20,26,27] This limit retains the strong-correlation effects that arise from trying to simultaneously minimize both the kinetic energy and the potential energy.

The many-body problem is solved by mapping it onto an auxiliary impurity problem[28,29] in a time-dependent field that mimics the hopping of an electron onto a site at time τ and off the site at a time τ'. The action for the impurity problem is found by integrating out all of the degrees of freedom of the other lattice sites in a path-integral formalism.[30] The result is an effective action

$$S_{\rm eff} = \sum_\sigma \int_0^\beta d\tau \int_0^\beta d\tau' c^\dagger_\sigma(\tau) G_0^{-1}(\tau - \tau') c_\sigma(\tau')$$
$$+ \sum_\sigma \int_0^\beta d\tau [g x(\tau) - \mu][c^\dagger_\sigma(\tau) c_\sigma(\tau) - 1]$$
$$+ \frac{1}{2} M \int_0^\beta d\tau [\Omega^2 x^2(\tau) + \dot{x}^2(\tau)] , \tag{4}$$

where G_0^{-1} is the "bare" Green's function that contains *all of the dynamical information of the other sites of the lattice.* The interacting Green's function, defined to be

$$G(i\omega_n) \equiv -\int_0^\beta d\tau e^{i\omega_n \tau} \frac{{\rm Tr}\langle e^{-\beta H} T_\tau c(\tau) c^\dagger(0)\rangle}{{\rm Tr}\langle e^{-\beta H}\rangle} ; \tag{5}$$

is determined by Dyson's equation

$$G_n^{-1} \equiv G^{-1}(i\omega_n) = G_0^{-1}(i\omega_n) - \Sigma(i\omega_n). \tag{6}$$

A self-consistency relation is required in order to determine the bare Green's function G_0. This is achieved by mapping the impurity problem onto the infinite-dimensional lattice, thereby equating the full Green's function for the impurity problem with the local Green's function for the lattice

$$G_{jj}(i\omega_n) = \sum_{\mathbf{k}} G(\mathbf{k}, i\omega_n)$$
$$= \sum_{\mathbf{k}} [i\omega_n + \mu - E(\mathbf{k}) - \Sigma(i\omega_n)]^{-1}$$
$$= F_\infty[i\omega_n + \mu - \Sigma(i\omega_n)]. \tag{7}$$

Here $F_\infty(z)$ is the scaled complementary error function of a complex argument[30]

$$F_\infty(z) \equiv \frac{1}{\sqrt{\pi}} \int_{-\infty}^{\infty} dy \frac{\exp(-y^2)}{z-y}$$
$$= -i\mathrm{sgn}[\mathrm{Im}(z)]\sqrt{\pi} e^{-z^2}$$
$$\times \mathrm{erfc}\{-i\mathrm{sgn}[\mathrm{Im}(z)]z\}. \quad (8)$$

The dynamics of the (local) impurity problem is identical to the dynamics of the Anderson impurity model[26,28–30,22] and is determined by employing a weak-coupling conserving approximation for the local problem and satisfying the self-consistency relation in Eq. (7).

It is important to note that, since one does not *a priori* know the bare Green's function G_0^{-1} in Eq. (4), one must iterate to determine a self-consistent solution for the Green's function of the infinite-dimensional lattice. This is done by performing self-consistent perturbation theory for the self-energy $\Sigma[G]$ within a conserving approximation, and then determining the new local Green's function from the approximate self-energy and Eq. (7). This process is iterated until convergence is achieved [the maximum variation of each $G(i\omega_n)$ is less than one part in 10^8 which typically takes between 5 and 30 iterations].

Static two-particle properties are also easily calculated since the irreducible vertex function is local.[31] The static susceptibility for CDW order is given by

$$\chi^{\mathrm{CDW}}(\mathbf{q}) \equiv \frac{1}{2N} \sum_{\mathbf{R}_j - \mathbb{R}_k \sigma\sigma'} e^{i\mathbf{q}\cdot(\mathbf{R}_j - \mathbf{R}_k)} T \int_0^\beta d\tau \int_0^\beta d\tau' [\langle n_{j\sigma}(\tau) n_{k\sigma'}(\tau')\rangle - \langle n_{j\sigma}(\tau)\rangle\langle n_{k\sigma'}(\tau')\rangle]$$
$$\equiv T \sum_{mn} \tilde{\chi}^{\mathrm{CDW}}(\mathbf{q}, i\omega_m, i\omega_n) = T \sum_{mn} \tilde{\chi}^{\mathrm{CDW}}_{mn}(\mathbf{q}) , \quad (9)$$

at each ordering wave vector $\mathbf{q}$. Dyson's equation for the two-particle Green's function becomes[22,31]

$$\tilde{\chi}^{\mathrm{CDW}}_{mn}(\mathbf{q}) = \tilde{\chi}^0_m(\mathbf{q})\delta_{mn} - T \sum_p \tilde{\chi}^0_m(\mathbf{q}) \Gamma^{\mathrm{CDW}}_{mp} \tilde{\chi}^{\mathrm{CDW}}_{pn}(\mathbf{q}) , \quad (10)$$

with $\Gamma^{\mathrm{CDW}}_{mn}$ the (local) irreducible vertex function in the CDW channel.

The bare CDW susceptibility $\tilde{\chi}^0_n(\mathbf{q})$ in Eq. (10) is defined in terms of the single-particle Green's function

$$\tilde{\chi}^0_n(\mathbf{q}) \equiv -\frac{1}{N} \sum_{\mathbf{k}} G_n(\mathbf{k}) G_n(\mathbf{k}+\mathbf{q})$$
$$= -\frac{1}{\sqrt{\pi}} \frac{1}{\sqrt{1-X^2(\mathbf{q})}} \int_{-\infty}^{\infty} dy \frac{e^{-y^2}}{i\omega_n + \mu - \Sigma_n - y}$$
$$\times F_\infty \left[\frac{i\omega_n + \mu - \Sigma_n - X(\mathbf{q}) y}{\sqrt{1-X^2(\mathbf{q})}} \right] \quad (11)$$

and all of the wave-vector dependence is included in the scalar[28,32] $X(\mathbf{q}) \equiv \sum_{j=1}^d \cos \mathbf{q}_j / d$. The mapping $\mathbf{q} \mapsto X(\mathbf{q})$ is a many-to-one mapping that determines an equivalence class of wave vectors in the Brillouin zone. "General" wave vectors are all mapped to $X = 0$ since $\cos \mathbf{q}_j$ can be thought of as a random number between -1 and 1 for "general" points in the Brillouin zone. Furthermore, all possible values of X $(-1 \le X \le 1)$ can be labeled by a wave vector that lies on the diagonal of the first Brillouin zone extending from the zone center $(X = 1)$ to the zone corner $(X = -1)$. The presence of incommensurate order in the attractive Holstein model is restricted to a very narrow region of parameter space[21,33] so only the "antiferromagnetic" point $X = -1$ is considered for CDW order. The integral for $\tilde{\chi}^0_m(X)$ in Eq. (11) can then be performed analytically[28] $\tilde{\chi}^0_n(X = -1) = -G_n/(i\omega_n + \mu - \Sigma_n)$. The irreducible vertex function $\Gamma^{\mathrm{CDW}}_{mn}$ is calculated perturbatively from the dressed Green's functions in a conserving approximation (see below).

A similar procedure is used for the singlet s-wave SC channel. The corresponding definitions are as follows: The static susceptibility in the superconducting channel is defined to be

$$\chi^{\mathrm{SC}}(\mathbf{q}) \equiv \frac{1}{N} \sum_{\mathbf{R}_j - \mathbf{R}_k} e^{i\mathbf{q}\cdot(\mathbf{R}_j - \mathbf{R}_k)} T \int_0^\beta d\tau$$
$$\times \int_0^\beta d\tau' \langle c_{j\uparrow}(\tau) c_{j\downarrow}(\tau) c^\dagger_{k\downarrow}(\tau') c^\dagger_{k\uparrow}(\tau')\rangle$$
$$\equiv T \sum_{mn} \tilde{\chi}^{\mathrm{SC}}(\mathbf{q}, i\omega_m, i\omega_n) = T \sum_{mn} \tilde{\chi}^{\mathrm{SC}}_{mn}(\mathbf{q}) , \quad (12)$$

for superconducting pairs that carry momentum $\mathbf{q}$; Dyson's equation becomes

$$\tilde{\chi}^{\mathrm{SC}}_{mn}(\mathbf{q}) = \tilde{\chi}^{0\prime}_m(\mathbf{q})\delta_{mn} - T \sum_p \tilde{\chi}^{0\prime}_m(\mathbf{q}) \Gamma^{\mathrm{SC}}_{mp} \tilde{\chi}^{\mathrm{SC}}_{pn}(\mathbf{q}) , \quad (13)$$

with $\Gamma^{\mathrm{SC}}_{mn}$ the corresponding irreducible vertex function for the SC channel; the bare pair field susceptibility becomes

$$\tilde{\chi}^{0\prime}_n(\mathbf{q}) \equiv \frac{1}{N} \sum_{\mathbf{k}} G_n(\mathbf{k}) G_{-n-1}(-\mathbf{k}+\mathbf{q})$$
$$= \frac{1}{\sqrt{\pi}} \frac{1}{\sqrt{1-X^2(\mathbf{q})}} \int_{-\infty}^{\infty} dy \frac{e^{-y^2}}{i\omega_n + \mu - \Sigma_n - y}$$
$$\times F_\infty \left[\frac{i\omega_{-n-1} + \mu - \Sigma_{-n-1} - X(\mathbf{q}) y}{\sqrt{1-X^2(\mathbf{q})}} \right] \quad (14)$$

with the special value $\tilde{\chi}^{0\prime}_n(X = 1) = -\mathrm{Im}G_n/\mathrm{Im}(i\omega_n - \Sigma_n)$ for the SC pair that carries no net momentum; and

finally the irreducible vertex function is also determined in the conserving formalism (see below).

At this point the transition temperature of the infinite-dimensional Holstein model is found by calculating the temperature at which the relevant susceptibility diverges (CDW or SC).

Section II contains the comparison of QMC exact solutions to ME theory and the second-order conserving approximation for the Holstein model. Analytical expressions for the change in T_c due to vertex corrections are given for the SC channel. Section III includes the application of conserving approximations to the attractive Hubbard model at half filling. Truncated conserving approximations through fourth order are compared to the different fluctuation-exchange approximations and the exact QMC solutions. Conclusions are presented in Sec. IV.

II. HOLSTEIN MODEL

There are two different types of approximations that are generally made for the electron-phonon interaction: the first method is a truncated conserving approximation that includes all vertex corrections to a finite order and is valid for all values of the phonon frequency;[15,21,33,12] the second method is ME theory in which vertex corrections are neglected, but the phonon propagator is dressed to all orders.[3,4,34] These two methods are compared and contrasted in Figs. 1 and 2. Figure 1(a) shows the self-energy for a conserving approximation through second order. The self-energy includes, respectively, the Hartree term (which is a constant and can be reabsorbed into the chemical potential), the Fock term, the second-order term that dresses the phonon propagator, and the lowest-order vertex correction. Figure 1(b) displays the corresponding self-consistent equations for ME theory: the self-energy includes the Hartree term (which can once again be reabsorbed into the chemical potential) and the Fock term (which is calculated with the *dressed* phonon propagator[34]). The dressed phonon propagator satisfies Dyson's equation [Fig. 1(c)].

To be more explicit, the self-energy for the second-order conserving approximation is

$$\Sigma_n(\text{cons}) = -g^2T\sum_r D_{n-r}G_r + g^4T^2\sum_{rs}[-2D_{n-r}+D_{r-s}] \times D_{n-r}G_rG_sG_{n-r+s}\ , \tag{15}$$

which includes the Fock diagram contribution and the two second-order contributions in Fig. 1(a). The bare phonon propagator $D_l \equiv D(i\nu_l)$ in Eq. (15) is given by

$$D_l = -\frac{1}{M(\Omega^2+\nu_l^2)}\ , \tag{16}$$

for each (bosonic) Matsubara frequency $\nu_l \equiv 2l\pi T$. On the other hand, in ME theory, the self-energy satisfies

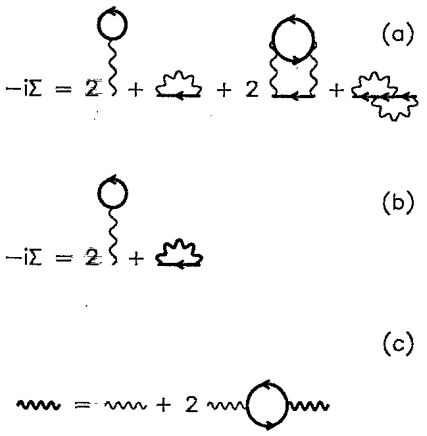

FIG. 1. Dyson equations for the self-energy of the Holstein model. The thick solid lines denote the *dressed* (electronic) Green's function and the thin wavy lines denote the phonon propagator. The self-energy (expanded out to second order in a conserving approximation) is depicted in (a) and includes the Hartree and Fock contributions, the second-order dressing of the phonon line and the lowest-order vertex correction. The self-consistent equation for the self-energy in Migdal-Eliashberg theory is shown in (b). The thick wavy line is the dressed phonon propagator which satisfies the Dyson equation in (c).

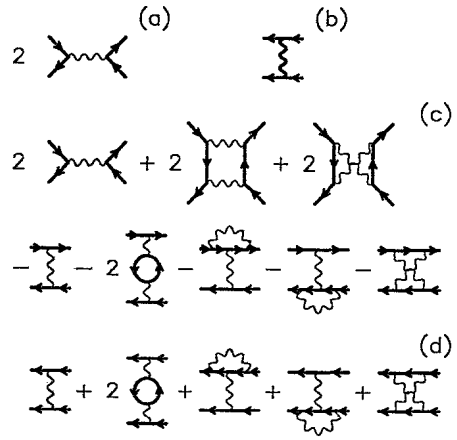

FIG. 2. The irreducible vertex functions in the CDW and SC channels. The CDW irreducible vertex function for ME theory is shown in (a). Note that the phonon propagator is *bare* in (a). The SC irreducible vertex function for ME theory appears in (b). Note that the phonon propagator is dressed here. The CDW irreducible vertex function for the second-order conserving approximation is shown in (c). Note that the vertex corrections (exchange diagrams) modify the interaction *to lowest order* in the CDW channel. The SC irreducible vertex function for the second-order conserving approximation is shown in (d). The vertex corrections first enter at second order in the SC channel.

$$\Sigma_n(\mathrm{ME}) = g^2 T \sum_r \frac{G_r}{M(\Omega^2+\nu_{n-r}^2)+\Pi_{n-r}} ,$$

$$\Pi_l \equiv 2g^2 T \sum_r G_{l+r} G_r , \tag{17}$$

with Π_l the phonon self-energy (evaluated in the limit where vertex corrections are neglected).

The self-consistency step involves determining a new local Green's function G_n from the integral relation in Eq. (7) with the approximate self-energy of Eq. (15) or Eq. (17). This process is repeated until the maximum deviation in the local Green's function is less than one part in 10^8.

Once the Green's functions and self-energies have been determined, the irreducible vertex functions can be calculated for the CDW or SC channels. The vertices are simple in the ME theory: the irreducible vertex in the CDW channel satisfies [see Fig. 2(a)]

$$\Gamma_{mn}^{\mathrm{CDW}}(\mathrm{ME}) = 2U ; \tag{18}$$

and the irreducible vertex function in the SC channel satisfies [see Fig. 2(b)]

$$\Gamma_{mn}^{\mathrm{SC}}(\mathrm{ME}) = -g^2 \frac{1}{M(\Omega^2+\nu_{m-n}^2)+\Pi_{m-n}} . \tag{19}$$

The phonon propagator in the CDW vertex is the *bare* propagator to avoid a double counting of diagrams.

The irreducible vertex functions acquire more structure in the second-order conserving approximation. In the CDW channel [see Fig. 2(c)] one must include both direct and exchange diagrams as well as the vertex corrections. The result is

$$\begin{aligned}\Gamma_{mn}^{\mathrm{CDW}}(\mathrm{cons}) = {} & 2U - 2U^2 T \sum_r [G_r G_{m-n+r} + G_r G_{m+n-r}] \left[\frac{\Omega^2}{\Omega^2+\nu_{n-r}^2}\right]^2 \\ & -U \frac{\Omega^2}{\Omega^2+\nu_{m-n}^2} - 2U^2 T \sum_r G_r G_{m-n+r} \frac{\Omega^2}{\Omega^2+\nu_{m-n}^2} \left[\frac{\Omega^2}{\Omega^2+\nu_{m-n}^2} - \frac{\Omega^2}{\Omega^2+\nu_{n-r}^2}\right] \\ & +U^2 T \sum_r G_r G_{m+n-r} \frac{\Omega^2}{\Omega^2+\nu_{m-r}^2} \frac{\Omega^2}{\Omega^2+\nu_{n-r}^2} .\end{aligned} \tag{20}$$

Note that the vertex corrections (arising from the first-order exchange diagrams) modify the *interaction* in the CDW channel so that it properly interpolates between the zero-frequency limit $\Gamma^{\mathrm{CDW}} \to 2U$ and the infinite-frequency limit $\Gamma^{\mathrm{CDW}} \to U$. At an intermediate phonon frequency, the CDW interaction strength has a complicated temperature dependence. In the SC channel [see Fig. 2(d)] one finds

$$\begin{aligned}\Gamma_{mn}^{\mathrm{SC}}(\mathrm{cons}) = {} & U \frac{\Omega^2}{\Omega^2+\nu_{m-n}^2} + U^2 T \sum_r G_r G_{m-n+r} \frac{\Omega^2}{\Omega^2+\nu_{m-n}^2} \left[2\frac{\Omega^2}{\Omega^2+\nu_{m-n}^2} - \frac{\Omega^2}{\Omega^2+\nu_{n-r}^2} - \frac{\Omega^2}{\Omega^2+\nu_{m+r+1}^2}\right] \\ & -U^2 T \sum_r G_r G_{m+n+r+1} \frac{\Omega^2}{\Omega^2+\nu_{m+r+1}^2} \frac{\Omega^2}{\Omega^2+\nu_{n+r+1}^2} .\end{aligned} \tag{21}$$

As the transition temperature (to a CDW-ordered state or a SC-ordered state) is approached from above, the susceptibility (in the relevant channel) diverges. Therefore, one can determine the transition temperature by finding the temperature where the scattering matrix (in the relevant channel)

$$T_{mn} = -T\Gamma_{mn}\chi_n^0 , \tag{22}$$

has unit eigenvalue.[35] In general, the eigenvector corresponding to the maximum eigenvalue of the scattering matrix is symmetric with respect to a change in sign of the Matsubara frequency (for the SC channel or for the CDW channel at half filling).

At half filling the Holstein model interaction is particle-hole symmetric, so the Green's functions and self-energies are purely imaginary and the vertices are real. The self-energy can be expressed by $\Sigma(i\omega_n) \equiv i\omega_n Z(i\omega_n)$, with $Z(i\omega_n)$ the renormalization function for the self-energy. At half filling, both $\chi_m^0(X=-1)$ and $\chi_m^{0\prime}(X=1)$ are also even functions of the Matsubara frequency, so the only contribution of the irreducible vertex function to the eigenvalue of the scattering matrix comes from the even Matsubara frequency component $[\Gamma_{m,n}+\Gamma_{-m-1,n}]/2$.

In order to judge the accuracy of these approximate methods for the electronic self-energy and the irreducible vertex functions, it is necessary to compare them to the exact results. The best way to do this would be to directly compare the perturbative results to the exact QMC results. Unfortunately, there are no available QMC data to do this. However, it has been well established that the iterated perturbation theory (IPT) of Georges and Kotliar[30] yields accurate results for the electronic self-energy of the Hubbard model (by direct comparison with the QMC results[24]) as long as the system is at half filling. The IPT is identical to the second-order conserving approximation, except that the perturbation theory is strictly truncated to second order in U.

A comparison of the approximations to the IPT results for the electronic self-energy and a comparison of the approximations for one column of the irreducible vertex

function in the CDW channel are made in Figs. 3 and 4 for two different interaction strengths at half filling. The phonon frequency is set to be approximately one-eighth of the effective bandwidth ($\Omega/t^* = 0.5$) as was done in the QMC solutions.[21] The energy cutoff is set to include 256 positive Matsubara frequencies for the perturbative approximations.

At weak coupling ($g = 0.4$, Fig. 3), the second-order conserving approximation clearly provides a more accurate approximation to the electron self-energy (under the assumption that the IPT is accurate). One expects the exact irreducible vertex function to be a frequency-dependent interaction, so the second-order conserving approximation is probably more accurate here too [the CDW vertex for the ME theory has no frequency dependence as shown in Eq. (18)].

An underestimation of the self-energy causes an overestimation of the transition temperature and vice versa. Similarly, an underestimation of the magnitude of the irreducible vertex will cause an underestimation of T_c (and vice versa). Since the ME theory overestimates the self-energy and overestimates the CDW vertex (because there is no weakening of the CDW vertex at small frequency transfers), it is difficult to predict whether or not ME theory will overestimate T_c. In the same fashion we do not know whether or not the second-order conserving ap-

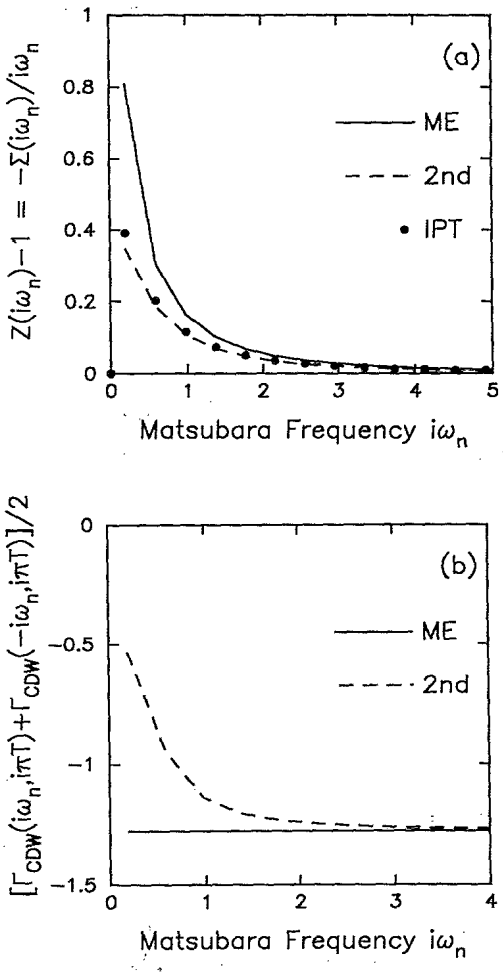

FIG. 3. Comparison of the ME theory (solid line) to the second-order conserving approximation (dashed line) for the Holstein model at half filling with phonon frequency $\Omega = 0.5t^*$, interaction strength $g = 0.4t^*$, and temperature $T = t^*/16$. This example is generic for the weak-coupling limit. In (a) the self-energy renormalization function $Z(i\omega_n) - 1$ is plotted against the Matsubara frequency and compared to the IPT (solid dots). In (b) the symmetric combination of the first column of the irreducible vertex function in the CDW channel is shown. Note that the second-order conserving approximation is clearly superior to ME theory in the limit of weak coupling.

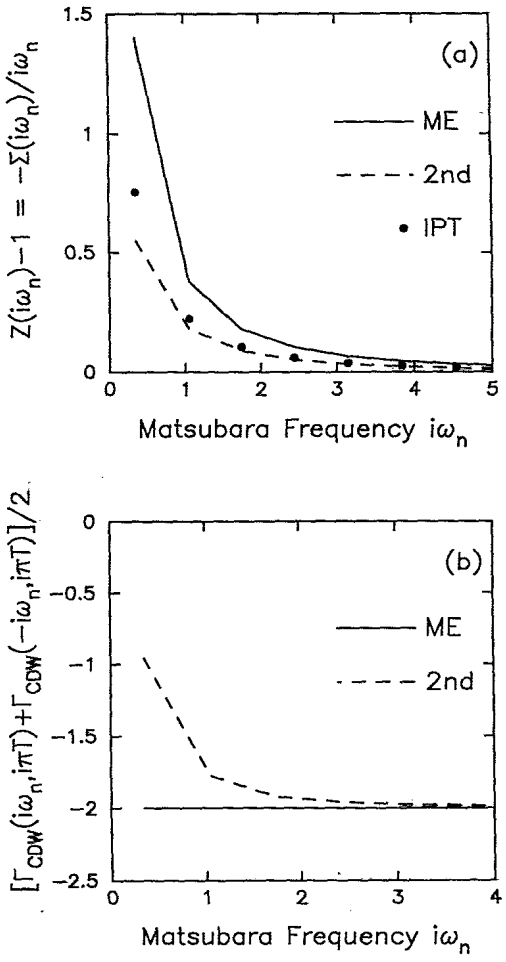

FIG. 4. Comparison of the ME theory (solid line) to the second-order conserving approximation (dashed line) for the Holstein model at half filling with phonon frequency $\Omega = 0.5t^*$, interaction strength $g = 0.5t^*$, and temperature $T = t^*/9$. This example is generic for the transition region to the strong-coupling limit. The self-energy renormalization function (a) and the irreducible vertex function in the CDW channel (b) are both pictured. In (a) the self-energy is compared to the IPT (solid dots). Note that in the limit where the strong-coupling effects begin to manifest themselves, the ME theory is becoming a more accurate approximation, or, put in other words, the total effect of vertex corrections is *reduced* as the interaction strength increases.

proximation will overestimate T_c since the magnitude of the exact vertex is not known.

As the coupling strength is increased to the point where a double-well structure began to develop in the effective phonon potential of the QMC simulations[21] ($g = 0.5$, Fig. 4) one can see strong-coupling effects becoming more important. Surprisingly, ME theory is becoming a more accurate approximation to the self-energy here. Stated in other words, as the coupling strength increases, the effect of vertex corrections is reduced.[11] Unfortunately, the self-consistent equations for the ME theory become unstable to an iterative solution as the coupling strength is increased further.

At half filling, the Holstein model always has a transition to a CDW-ordered phase at $\mathbf{q} = (\pi, \pi, \pi, ...)$ ($X = -1$). The transition temperature to this commensurate CDW is plotted in Fig. 5 as a function of the interaction strength. The second-order conserving approximation is compared to ME theory and the QMC simulations.[21] The conserving approximation is much more accurate at weak coupling[16,17,12] (ME theory predicts a transition temperature that is an order of magnitude higher than the QMC and conserving approximation results at the lowest value of the coupling considered) because the inclusion of the first-order exchange diagrams produces the correct interaction and the inclusion of the second-order terms produces the correct prefactor. However, ME theory does display the proper qualitative behavior of developing a peak in T_c as the interaction strength increases. This feature is not reproduced by the truncated conserving approximation.

As the system is doped away from half filling, the CDW instability remains locked at the commensurate point ($X = -1$) until it gives way to a SC instability (incommensurate order may appear in a very narrow region of phase space near the CDW-SC phase boundary[21,33] but is neglected here). In Fig. 6, the phase diagram of the Holstein model is plotted for two values of the interaction strength ($g = 0.4$, $g = 0.5$). The weak-coupling QMC data ($g = 0.4$) are reproduced most accurately by the second-order conserving approximation, as expected from the comparison of the self-energy and the vertices in Fig. 3. The SC transition is reproduced remarkably well, because the underestimation of the self-energy [Fig. 3(a)] must be compensated by an underestimation of the SC vertex. The critical concentration for the CDW-SC phase boundary is also more accurately determined by the conserving approximation. Note that the difference between the SC transition temperature calculated with ME theory and with the second-order conserving approximation explicitly shows the lowest-order effect of vertex corrections. The vertex corrections lower T_c by about a factor of 2 at the phase boundary, but are reduced as the doping increases.

At the stronger coupling strength ($g = 0.5$) ME theory reproduces the CDW transition temperature very accu-

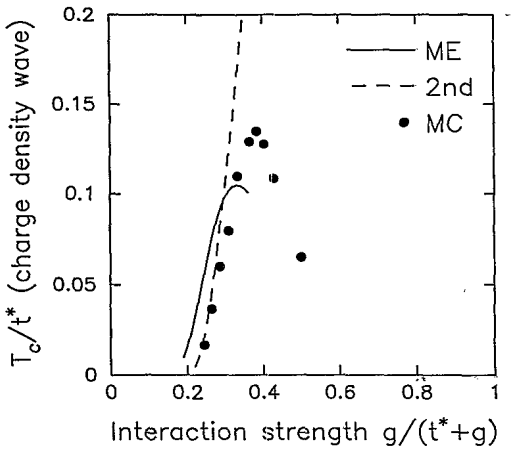

FIG. 5. Transition temperature to the CDW-ordered state at half filling in the Holstein model at an intermediate phonon frequency ($\Omega = 0.5t^*$). The ME theory (solid line) is compared to the second-order conserving approximation (dashed line) and the QMC results (solid dots). Note that the vertex corrections are very important in the CDW channel and that only the second-order conserving approximation produces the correct result in the weak-coupling limit. ME theory does, however, display the correct qualitative behavior of developing a peak in T_c as a function of interaction strength.

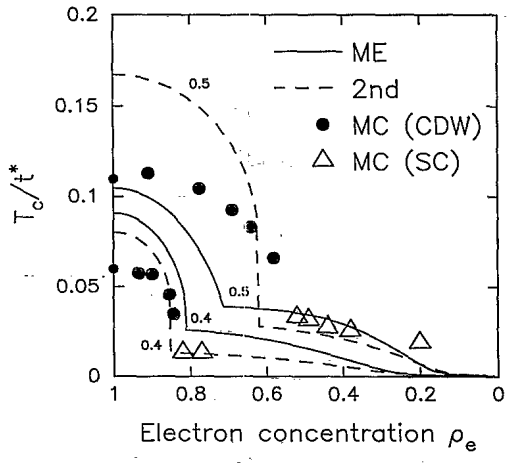

FIG. 6. Phase diagram of the Holstein model with $\Omega = 0.5t^*$ at two different coupling strengths ($g = 0.4, 0.5$). The solid dots are the QMC solutions with CDW order, and the open triangles are the QMC results with SC order. The kinks in the solid (ME) and dashed (second-order conserving approximation) lines occur at the CDW-SC phase boundaries. In the weak-coupling limit ($g = 0.4$) the second-order conserving approximation is superior to the ME theory and is quite accurate for the SC transition. The difference between the ME results and the second-order conserving approximation shows explicitly the lowest-order effects of vertex corrections upon the SC transition temperature. The effect of vertex corrections is reduced as the filling is reduced. ME theory is quantitatively more accurate in determining T_c for the stronger coupling strength ($g = 0.5$) but the second-order conserving approximation is superior in determining the CDW-SC phase boundary. Clearly both approximations are failing at such a large value of the interaction strength.

rately at half filling, but not the doping dependence of T_c. It does manage to reproduce the transition temperature in the SC sector quite well, but the second-order conserving approximation is superior at determining the CDW-SC phase boundary. Clearly both approximation methods are inadequate at this large a value of the coupling strength.

Up to this point we have concentrated on one value of the phonon frequency and have compared the numerical solution of the self-consistent perturbation theory with the numerically exact QMC solutions. In the limit of weak coupling ($|U| \to 0$), the transition temperature approaches zero ($T_c \to 0$) and the leading behavior of T_c can be determined analytically.[16,17,12,33] We will concentrate on the SC channel only, because the analytical techniques are not as accurate for the CDW channel.

In the limit $T \to 0$, the self-energy satisfies

$$\lim_{T\to 0}[i\omega_n + \mu - \Sigma(i\omega_n)] = \bar{\mu} + i\omega_n Z \ , \tag{23}$$

where the renormalized chemical potential is

$$\bar{\mu} = \mu - \lim_{T\to 0} \mathrm{Re}\Sigma(i\omega_n) = \mu - U\rho_e + O(U^2) \ , \tag{24}$$

and the renormalization function is

$$\begin{aligned} Z &= Z(0) \\ &= 1 + |U| \int_0^\infty dy \frac{\rho(y+\mu)+\rho(-y+\mu)}{2} \frac{\Omega}{(\Omega+y)^2} \\ &\quad + O(U^2) \ . \end{aligned} \tag{25}$$

Here $\rho(y) \equiv \exp(-y^2)/\sqrt{\pi}$ is the noninteracting density of states (DOS) in infinite dimensions. The irreducible vertex in the SC channel [Eq. (21)] becomes

$$\Gamma^{\mathrm{SC}}_{mn} = -\frac{\Omega^2}{\Omega^2 + \nu^2_{m-n}} |U|[1 + 2|U|I_1] + U^2 I_2 + O(U^3) \ , \tag{26}$$

with I_1 and I_2 two smooth temperature-dependent integrals that can be approximated by their zero-temperature limit:

$$I_1 \equiv -\frac{1}{2\pi} \int_{-\infty}^{\infty} dy F^2_\infty(iy+\mu) \frac{y^2}{\Omega^2+y^2} + O(U) \ , \tag{27}$$

$$I_2 \equiv -\frac{1}{2\pi} \int_{-\infty}^{\infty} dy F^2_\infty(iy+\mu) \frac{\Omega^4}{(\Omega^2+y^2)^2} + O(U) \ . \tag{28}$$

The bare susceptibility becomes

$$\chi^{0\prime}_n(X=1) = -\frac{\mathrm{Im}F_\infty(i\omega_n Z + \bar{\mu})}{\omega_n Z} + O(U^2) \ , \tag{29}$$

for the electron pairs that carry no net momentum.

In the square-well approximation,[36,2] the smooth temperature dependence of the SC vertex is replaced by a sharp cutoff at a characteristic frequency ω_c,

$$\frac{\Omega^2}{\Omega^2 + \nu^2_{m-n}} \to \theta(\omega_c - |\omega_m|)\theta(\omega_c - |\omega_n|) \ , \tag{30}$$

with $\theta(x)$ the unit step function. The scattering matrix [in Eq. (22)] then becomes

$$\begin{aligned} T_{mn} = -T[&\theta(\omega_c - |\omega_m|)\theta(\omega_c - |\omega_n|)|U|(1 + 2|U|I_1) \\ &- U^2 I_2] \frac{\mathrm{Im}F_\infty(i\omega_n Z + \bar{\mu})}{\omega_n Z} \ . \end{aligned} \tag{31}$$

The SC transition temperature is now determined by solving the matrix eigenvalue equation $\sum_n T_{mn}\phi_n = \phi_m$.

The eigenvector ϕ_m can be chosen to be of the form $\phi_m = 1 + a\theta(\omega_c - |\omega_m|)$ in the square-well approximation, so that the matrix eigenvalue equation is reduced to two coupled algebraic equations

$$\begin{aligned} a &= \frac{\rho(\mu)|U|}{Z}(1 + 2|U|I_1)(1+a)R \ , \\ 1 &= -\frac{\rho(\mu)U^2}{Z} I_2(aR + S) \ , \end{aligned} \tag{32}$$

with R and S defined by

$$R \equiv -\frac{T}{\rho(\mu)} \sum_{|\omega_n|<\omega_c} \frac{\mathrm{Im}F_\infty(i\omega_n Z + \bar{\mu})}{\omega_n} \ , \tag{33}$$

$$S \equiv -\frac{T}{\rho(\mu)} \sum_{n=-\infty}^{\infty} \frac{\mathrm{Im}F_\infty(i\omega_n Z + \bar{\mu})}{\omega_n} \ . \tag{34}$$

The infinite summation over Matsubara frequencies can be performed in the standard fashion[2] to yield

$$\begin{aligned} S &= \frac{1}{2} \int_{-\infty}^{\infty} \frac{dy}{y} \frac{\rho(y+\bar{\mu})}{\rho(\mu)} \tanh \frac{y}{2ZT_c} \\ &= \ln \frac{1}{2ZT_c} \\ &\quad + \int_0^\infty \frac{dy}{y} \left(\tanh y - 1 + \frac{\rho(y+\bar{\mu}) + \rho(-y+\bar{\mu})}{2\rho(\mu)} \right) \ , \end{aligned} \tag{35}$$

while the truncated summation can be expressed in an integral form[10]

$$\begin{aligned} R &= S - \frac{1}{\pi\rho(\mu)} \int_{\omega_c}^\infty \frac{dy}{y} \mathrm{Im}F_\infty(iyZ + \bar{\mu}) \\ &= S - \frac{2}{\pi} \int_0^\infty \frac{dy}{y} \frac{\rho(y+\bar{\mu}) + \rho(-y+\bar{\mu})}{2\rho(\mu)} \tan^{-1} \frac{y}{Z\omega_c} \end{aligned} \tag{36}$$

if the transition temperature is much less than the cutoff frequency ($T_c \ll \omega_c$).

The coupled algebraic equations [in Eq. (32)] are then solved by

$$\frac{Z}{\rho(\mu)|U|} = [1 + |U|(2I_1 - I_2)]S + (1 + 2|U|I_1)(R - S) \ , \tag{37}$$

to order $|U|$. The limiting form of the transition temperature is now found by substituting Eqs. (35) and (36) for R and S into Eq. (37) and solving for T_c. The result is

$$T_c = \exp\left(-\frac{1}{\rho(\mu)|U|}\right) f_{\text{phonon}} f_{\text{electron}} f_{\text{DOS}} f_{\text{vertex}} , \quad (38)$$

which includes the interaction term and the constant prefactors. The constant terms arise from the phonon self-energy, the electron self-energy, the nonconstant DOS, and the vertex corrections.

The phonon self-energy correction is

$$f_{\text{phonon}} = \exp\left[-\frac{1}{\pi\rho(\mu)}\text{Re}\int_{-\infty}^{\infty} dy F_{\infty}^2(iy+\mu)\right]$$

$$= \exp\left[\sqrt{2}\int_{-\infty}^{\infty}\frac{dw\,\rho(w)}{w\;\rho(\mu)}\text{erf}(w+\sqrt{2}\mu)\right] , \quad (39)$$

and is independent of the phonon frequency. This correction factor is normally included in the definition of the electron-phonon interaction strength λ,

$$\lambda \equiv \rho(\mu)|U|\left[1-\frac{|U|}{\pi}\text{Re}\int_{-\infty}^{\infty} dy F_{\infty}^2(iy+\mu)\right] , \quad (40)$$

of the ME theory formalism.

The electron self-energy factor satisfies

$$f_{\text{electron}} = \exp\left[-\int_0^{\infty} dy e^{-y^2}\cosh(2\mu y)\frac{\Omega}{(\Omega+y)^2}\right] , \quad (41)$$

which approaches the standard ME theory result of $f_{\text{electron}} \to e^{-1}$ as $\Omega \to 0$ and approaches the standard Hubbard model result of $f_{\text{electron}} \to 1$ as $\Omega \to \infty$.

The nonconstant DOS factor is

$$f_{\text{DOS}} = \frac{1}{2}\exp\int_0^{\infty}\frac{dy}{y}\left[\tanh y - 1\right.$$

$$\left. + e^{-y^2}\cosh(2\mu y)\left(1-\frac{2}{\pi}\tan^{-1}\frac{y}{\omega_c}\right)\right] , \quad (42)$$

which depends on the square-well cutoff frequency ω_c. In the limit $\omega_c \to 0$, f_{DOS} approaches the ME theory result of $1.14\omega_c$, whereas in the limit $\omega_c \to \infty$, f_{DOS} approaches the Hubbard model result[33]

$$\lim_{\omega_c\to\infty} f_{\text{DOS}} = 0.85\exp\left[2\int_0^{\infty}\frac{dy}{y}e^{-y^2}\sinh^2\mu y\right]$$

$$= 0.85\exp\left[\sqrt{\pi}\int_0^{\mu} dy e^{y^2}\text{erf}(y)\right] . \quad (43)$$

Note that, once the phonon energy scale is larger than the electronic energy scale, it is the band structure (not ω_c) that determines the DOS prefactor.

Finally, the vertex correction factor becomes

$$f_{\text{vertex}} = \exp\left[\frac{1}{\pi\rho(\mu)}\text{Re}\int_{-\infty}^{\infty} dy F_{\infty}^2(iy+\mu)\right.$$

$$\left.\times\frac{\Omega^2}{\Omega^2+y^2}\left(1+\frac{1}{2}\frac{\Omega^2}{\Omega^2+y^2}\right)\right] , \quad (44)$$

which approaches 1 as $\Omega \to 0$. In the high-frequency limit, the vertex corrections cancel the phonon self-energy corrections and yield

$$\lim_{\Omega\to\infty} f_{\text{phonon}} f_{\text{vertex}}$$

$$= \exp\left[-\frac{1}{\sqrt{2}}\int_{-\infty}^{\infty}\frac{dw}{w}\frac{\rho(w)}{\rho(\mu)}\text{erf}(w+\sqrt{2}\mu)\right] , \quad (45)$$

which reproduces van Dongen's result[16] $f_{\text{phonon}} f_{\text{vertex}} = \exp[-\sqrt{2}\ln(1+\sqrt{2})]$ at half filling ($\mu = 0$). In the infinite-frequency limit (attractive Hubbard model), the vertex corrections always reduce T_c.

The effects of vertex corrections upon the superconducting transition temperature in the weak-coupling limit are displayed in Fig. 7(a). The vertex correction factor, $f_{\text{vertex}} = T_c(\text{vertex})/T_c(\text{no vertex})$, is plotted against the phonon frequency for eight different electron concentrations. At half filling, the vertex corrections sharply reduce T_c, so that T_c calculated with vertex corrections is a factor of 2 lower than T_c calculated without vertex corrections at $\Omega = 0.13t^*$ (or, since the effective electronic bandwidth is approximately $W = 4t^*$, when $\Omega/W = 0.03$). Therefore, vertex corrections should play an important role in $Ba_{1-x}K_xBiO_3$ where $\Omega/W = 0.02$.

As the system is doped away from half filling the effect of the vertex corrections is reduced (as was already seen in Fig. 6), until a critical electron concentration ($\rho_c \approx 0.2$) is reached where the vertex corrections initially cause an *enhancement* to T_c. This enhancement occurs because the electronic Green's functions have a larger real part than imaginary part, which causes the integrand in Eq. (44) to change sign for small y. This enhancement will not be seen in standard ME theory with a constant DOS, because the Green's functions are chosen to be purely imaginary in that case. As the phonon frequency is increased to a large enough value, the vertex corrections will once again reduce T_c, because they always cause a reduction in the limit $\Omega \to \infty$ [see Eq. (45)].

The square-well cutoff frequency ω_c should vanish as the phonon frequency vanishes, and should become infinite as the phonon frequency becomes infinite. The cutoff frequency is chosen to be three-fifths of the phonon frequency ($\omega_c = 0.6\Omega$), so that the proper limiting behavior is attained[2,12,16] as $\Omega \to 0$ and $\Omega \to \infty$. The prefactor to the SC transition temperature in Eq. (38) is plotted in Fig. 7(b) for eight different electron concentrations. Note that there is an optimal phonon frequency where the SC response is maximal, which shifts from a low frequency at half filling to higher frequencies as the electron concentration is reduced. The optimal phonon frequency is usually smaller than the effective bandwidth ($W = 4t^*$).

In general, one must expand the free energy through second order[16,17] to properly determine T_c in the limit

$|U| \to 0$. The miracle of ME theory is that a first-order calculation with dressed phonons properly determines T_c in the limit $\Omega \to 0$. In the CDW channel, the vertex corrections modify both the interaction strength and the prefactor, while in the SC channel, only the prefactor is modified. It is this robustness of the SC channel to the effects of vertex corrections that explains the success of ME theory for low-temperature superconductors.

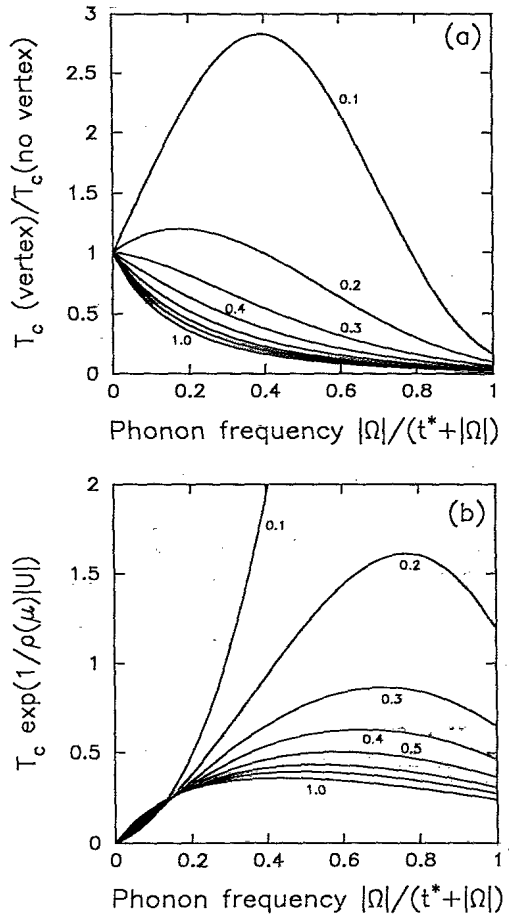

FIG. 7. Plot of the lowest-order effect of vertex corrections on the SC transition temperature in the weak-coupling limit. In (a) the renormalization factor for the transition temperature calculated with vertex corrections divided by the transition temperature calculated without vertex corrections is plotted as a function of the phonon frequency. Eight different values of the electron density are plotted ($\rho_e = 0.1, 0.2, 0.3, 0.4, 0.5, 0.6, 0.7, 1.0$). Note that the vertex corrections always reduce T_c in the high-phonon-frequency limit, but that vertex corrections initially *enhance* T_c at low electron density ($\rho_e < 0.2$). At half filling (where the Green's functions are purely imaginary) vertex corrections will reduce T_c by a factor of 2 when $\Omega/W = 0.03$. In (b) the prefactor of the weak-coupling T_c formula is plotted against the phonon frequency for the same eight values of the electron density. The cutoff frequency has been chosen to satisfy $\omega_c = 0.6\Omega$. Note that there is always an optimal phonon frequency where the SC response will be the largest, and that this optimal phonon frequency increases as the electron concentration decreases.

III. HUBBARD MODEL

The Hubbard model in Eq. (3) is the infinite-frequency limit ($\Omega \to \infty$) of the Holstein model. The Hubbard model has an electron-electron interaction that only occurs between electrons with opposite spins. This happens because of the cancellation of the direct and exchange diagrams which causes all electron-electron interactions between like-spin particles to vanish. The perturbation theory becomes much simpler in the Hubbard model case, because of this reduction of diagrams, and can be performed to higher order. Here the truncated conserving approximation will be carried out to fourth order, and will be compared to the fluctuation-exchange (FLEX) approximation[15] to determine the best way to approximate the Hubbard model in the infinite-dimensional limit. Previous work has concentrated on second-order conserving approximations,[32,37] third-order conserving approximations,[12] or the FLEX approximation.[38]

One expects that a truncated approximation will be superior to an infinite summation of random-phase approximation (RPA) bubbles and particle-hole and particle-particle ladders because the many-body problem reduces to a self-consistently embedded Anderson impurity model, and the analysis of Yamada[39] has shown that the total fourth-order corrections to the self energy are an order of magnitude smaller and opposite in sign to the fourth-order contribution of the FLEX approximation. The irreducible vertex functions should have similar effects, but have not yet been analyzed in detail.

The diagrammatic expansion for self-energy (in a conserving approximation) of the Hubbard model is given in Fig. 8. The first line includes the first-order Hartree contribution (which is a constant that can be absorbed into a renormalized chemical potential), the second-order contribution, and the third-order particle-hole and particle-particle ladders. The second line contains the fourth-order contributions from the RPA bubbles and the particle-hole and particle-particle ladders. The third and fourth lines include all of the remaining fourth-order diagrams (the inclusion of the second-order self-energy into the dressed Green's function of the second-order diagram produces another fourth-order contribution to the self-energy, but this is automatically included in the self-consistency step of the conserving approximation). The FLEX approximation consists of the summation of all RPA bubbles, particle-hole ladders, and particle-particle ladders. The self-energy has already been determined on the real axis by Menge and Müller-Hartmann.[38] The FLEX approximation for the self-energy includes all contributions through third order in U (the first line of Fig. 8) but only a partial contribution of the fourth-order and higher-order terms (the second line of Fig. 8 plus the higher-order terms). An explicit formula for the electronic self-energy of the Hubbard model through fourth order is given in the Appendix. The corresponding formula for the FLEX approximation has been given before.[15,38]

The irreducible vertex functions are too cumbersome to represent diagrammatically, but an explicit formula for the CDW vertex is given in the Appendix. The cor-

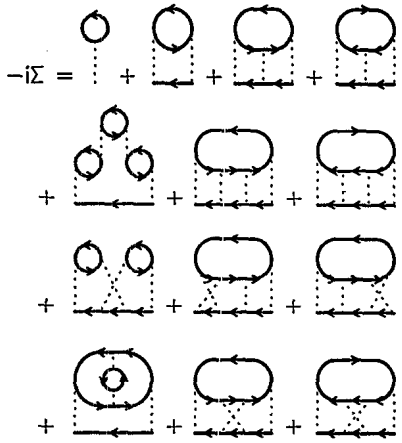

FIG. 8. Self-energy diagrams for the Hubbard model through fourth order. The thick solid lines denote the *dressed* electronic Green's functions, and the thin dotted lines are the Coulomb interaction. The first two lines contain all of the FLEX contributions truncated to fourth order. The last two lines are the remaining fourth-order diagrams. At half filling the odd-order contributions to Σ vanish, and each of the three fourth-order contributions on the same line yields the same contribution to Σ.

responding formula for the FLEX approximation has already been given.[15] An additional simplification is usually made for the FLEX approximation that neglects a large class of diagrams for the irreducible vertices (the so-called Aslamazov-Larkin diagrams,[40]) thereby including only those contributions to the irreducible vertex function that can be represented by functions of the bare particle-hole or bare particle-particle susceptibilities.[15] This simplified FLEX approximation will be denoted FLEX*.

Since the Hubbard model interaction is particle-hole symmetric, the half-filled band corresponds to $\mu = 0$, and the Green's functions are purely imaginary. The odd-order contributions to the self-energy all vanish and each of the fourth-order contributions on a given line in Fig. 8 is identical[39] (see the Appendix). Furthermore, it can be shown that the most complicated contributions to the irreducible vertex function in the CDW channel are odd under a change in the sign of the Matsubara frequency, and can be neglected in calculating the maximum eigenvalue of the scattering matrix, because only the even component of the irreducible vertex function enters (see the Appendix for details).

Note that, since the self-energy is an odd function of U at half filling, but the irreducible vertex function contains both even and odd powers of U, the only difference between a truncated conserving approximation of order $2n$ and of order $2n+1$ is that the irreducible vertex function is larger for the odd-order approximation. Therefore, we expect that an even-order approximation will underestimate the transition temperature (in weak coupling) and an odd-order approximation will overestimate T_c.

A comparison of the different approximation schemes is given in Figs. 9 and 10 for two different values of U. The second-order, third-order, and FLEX approximations all employ an energy cutoff of 256 positive Matsubara frequencies; the fourth-order approximation uses 64 positive Matsubara frequencies. In Fig. 9(a) the self-energy renormalization function is plotted for the three different approximations at $U = -t^*$ and compared to the highly accurate IPT.[30] Note that the fourth-order approximation virtually reproduces the IPT results, but that the FLEX approximation grossly overestimates the self-energy even though the coupling strength is not too

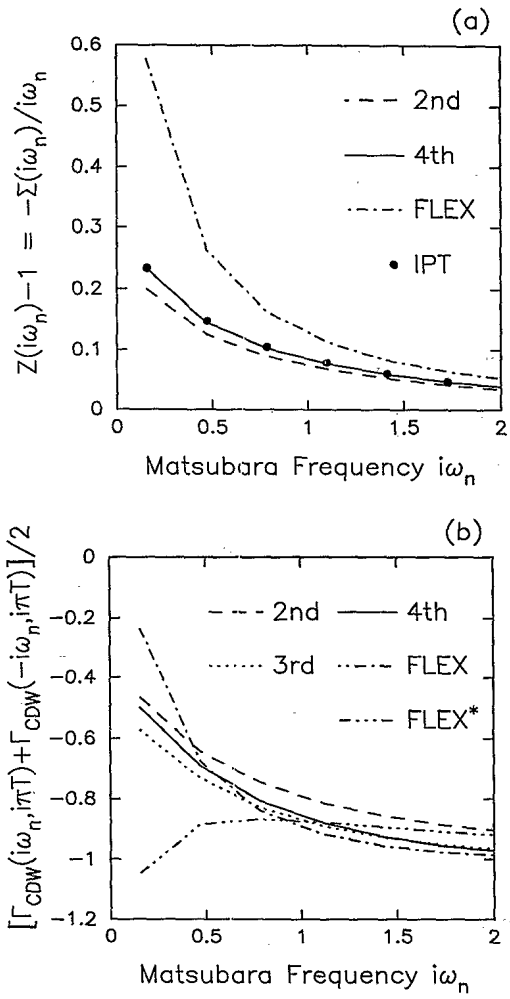

FIG. 9. Comparison of the different conserving approximations for the Hubbard model at half filling in the limit of weak coupling ($U = -t^*, T = t^*/20$). The second-order (dashed line), third-order (dotted line), and fourth-order (solid line) conserving approximations are compared to the full FLEX (chain dotted line) and the simplified FLEX* (chain triple dotted line). In (a) the self-energy renormalization function is plotted against Matsubara frequency and compared to the IPT (solid dots). In (b) the even component of the first column of the irreducible vertex function in the CDW channel is plotted. Clearly the fourth-order approximation is the best approximation in this limit. The FLEX approximation grossly overestimates the self-energy. The simplified FLEX* compensates for this by overestimating the vertex to produce a more accurate value for T_c.

large. In Fig. 9(b) the even component of one row of the irreducible vertex function for the CDW channel is compared for $U = -t^*$. All of the truncated conserving approximations are in reasonable agreement with each other; the FLEX approximation has the smallest magnitude at low Matsubara frequency. The simplified FLEX* grossly overestimates the magnitude of the vertex (in fact the FLEX* approximation produces the wrong qualitative behavior of the vertex). In general, the transition temperature calculated with the simplified FLEX* will be a more accurate approximation to the exact T_c than that calculated with the full FLEX, because the overestimation of the self-energy will be compensated for by the overestimation of the vertex in FLEX*. These results are similar to what White[41] found for the repulsive Anderson impurity model.

As the coupling strength is increased to $U = -2t^*$, the FLEX approximation becomes a more accurate approximation for the self-energy than the truncated conserving approximations [see Fig. 10(a)]. Clearly, the truncated conserving approximation must be performed to a high order to accurately reproduce the self-energy in the strongly correlated regime. The irreducible vertex function in the CDW channel is plotted in Fig. 10(b). The different approximations no longer agree well with each other, indicating that the perturbation theory is breaking down.

The transition temperature for the CDW transition at half filling in the attractive Hubbard model is plotted in Fig. 11 as a function of U. The truncated conserving approximations are doing quite well in the weak-coupling regime. The odd-order approximation overestimates T_c, while the even-order approximations underestimate T_c. The even-order approximations tend to be more accurate over a wider range of U than the odd-order approximation, but neither approximation properly reproduces the turnover in T_c as a function of U as seen in the QMC simulations.[22] Note also that all truncated approximations agree in the limit $U \to 0$, but that a first-order (RPA) calculation will be off by a factor of 3 in the weak-coupling limit.[16,17,12] The FLEX approximation does have the correct qualitative behavior of developing a peak in T_c as a function of U but the peak position and peak height are off by about an order of magnitude. The simplified FLEX* is, in general, a more accurate approximation than the full FLEX, but

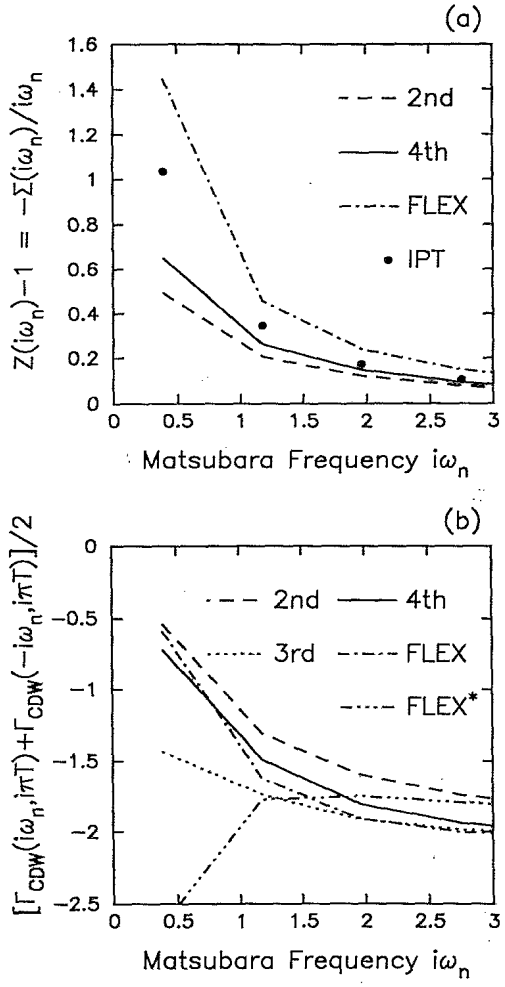

FIG. 10. Same as Fig. 9, but with a stronger value of the coupling ($U = -2t^*, T = t^*/8$). In this limit the FLEX approximation is superior for the self-energy, but the vertex *does not* appear to be reproduced accurately by any approximation.

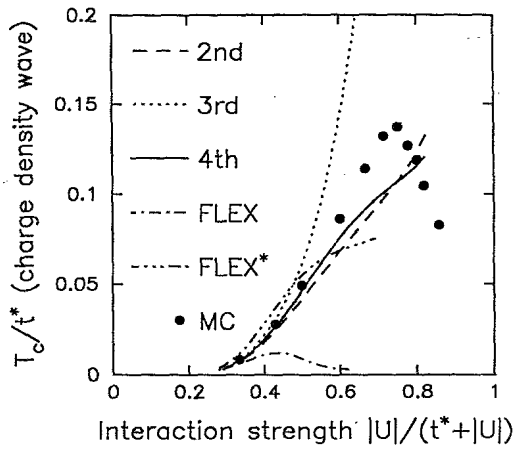

FIG. 11. Transition temperature to the CDW-ordered state in the Hubbard model at half filling. The second-order (solid line), third-order (dotted line), and fourth-order (solid line) conserving approximations are compared to the full FLEX (chain dotted line), the simplified FLEX* (chain triple dotted line), and the QMC results (solid dots). Note that the odd-order approximations overestimate T_c, the even-order approximations underestimate T_c, and that one has to go to very high order to reproduce the peak in the transition temperature as a function of the interaction strength. The FLEX approximation displays the correct qualitative behavior of developing a peak, but is off by an order of magnitude in the peak position and height. The simplified FLEX* yields a quantitatively more accurate approximation, but is poorer in the limit of weak coupling because it does not include all of the third-order contributions properly.

becomes unstable if U is increased too far. The FLEX* does not agree as well with the QMC calculations (or with the other approximations) in the weak-coupling limit because the irreducible vertex function does not include all of the third-order contributions.

The reason why the truncated (even-order) conserving approximations do not approximate the self-energy (or the vertex) too accurately at moderate coupling, but are good approximations for the transition temperature at moderate coupling, is most likely due to a cancellation of the effect of an underestimation of the self-energy by an underestimation of the vertex in the calculation of T_c. This probably explains why the T_c curves do not turn over for the truncated approximations as well: the turnover must be arising from self-energy effects that are being underestimated here.

In summary, the truncated approximations tend to give better numerical agreement than an approximation that tries to sum an infinite series of diagrams (such as the FLEX). One must go to very high order to see a peak develop in T_c as a function of U and to have good quantitative agreement with the QMC results. It will be interesting to see if the removal of the infinite summation of diagrams in the conserving approximation produces an even better agreement with the QMC results (as was found for the Anderson impurity model[39]). The approximation will no longer be a conserving one, and will need to be generalized to move off half filling, but should be even more accurate. The fluctuation-exchange approximation seems to be a poor approximation, and should not be tried for the Holstein model; rather one should concentrate on generalizing Yamada's analysis for instantaneous interactions to one for retarded interactions to see whether or not one can improve upon the accuracy in that case too.

IV. CONCLUSIONS

Vertex corrections can be systematically incorporated into a weak-coupling theory of electron-phonon interactions. Expansions must be performed to second order in the effective electron-electron interaction in order to produce the correct behavior in the weak-coupling limit.[16,17] The miracle of Migdal-Eliashberg theory[3,4] is that a first-order calculation suffices (with dressed phonon propagators) in the small-phonon-frequency limit. Vertex corrections enter to lowest order in the CDW channel, modifying the interaction strength. They enter to higher order in the SC channel, and merely modify the prefactor of the weak-coupling T_c equation. This robustness of the SC channel to the effects of vertex corrections explains its remarkable success for low-temperature superconductors. Nevertheless, the effect of vertex corrections should be strong enough to be observable in materials such as $Ba_{1-x}K_xBiO_3$ and the doped fullerenes. It is possible that the effects of vertex corrections can even be detected in certain low-temperature superconductors such as Pb.

In general, vertex corrections will reduce the transition temperature; however there is a small parameter regime at low electron density where the vertex corrections actually cause an enhancement to the superconducting transition temperature. This occurs because the real parts of the Green's functions are larger than the imaginary parts for small imaginary frequency and low electron concentration. At high enough phonon frequency, or large enough electron density, the vertex corrections will lower T_c.

Truncated conserving approximations appear to be better approximations than infinite summation schemes such as the fluctuation-exchange approximation.[15] The electronic self-energy, the irreducible vertex functions, and the transition temperatures all appear to be better approximated by a truncated conserving approximation. The qualitative feature of the development of a peak in the transition temperature as a function of the interaction strength is, however, not reproduced by a truncated conserving approximation. Perhaps a completely truncated approximation (that is no longer conserving) will do even better at approximating properties of interacting electronic systems in infinite dimensions. Yamada[39] and White[41] found this to be so for the Anderson impurity model, and those techniques have been applied in infinite dimensions[30,24] to second order in U. What is needed is a way to generalize Yamada's work off half filling for both the self-energy and the irreducible vertex functions. Work in this direction is currently in progress.

In conclusion, a weak-coupling conserving approximation has been carried out for the attractive Holstein and Hubbard models that includes all effects of vertex corrections and nonconstant density of states. Agreement with the exact solutions is found to be excellent at weak coupling, but the qualitative feature of developing a peak in T_c as a function of the interaction strength is not reproduced. From this standpoint, a weak-coupling theory is much more difficult to control than a strong-coupling theory (perturbation theory in the kinetic energy). Analytic expressions for T_c in the SC channel have been explicitly derived, and they indicate that vertex corrections may be observable for some classes of low-temperature superconductors. Future work will include an examination of the ordered phase, a study of the effects of Coulomb repulsion, and a real materials calculation to look for the effects of vertex corrections in low temperature superconductors.

Note added in proof. After completion of this work I learned about a similar study applying the local approximation to the electron-phonon problem in two dimensions by H. R. Krishnamurthy, D. M. Newns, P. C. Pattnaik, C. C. Tsuei, and C. C. Chi, Phys. Rev. B **49**, 3520 (1994).

ACKNOWLEDGMENTS

I would like to thank N. E. Bickers, T. Devereaux, M. Jarrell, E. Nicol, R. Scalettar, and P. van Dongen for many useful discussions. I would especially like to thank D. Scalapino for his continued interest in this problem and for numerous discussions. This research is supported by the Office of Naval Research under Grant No. N00014-93-1-0495. Initial stages of this research were performed at the Institute for Theoretical Physics in Santa Barbara and were supported in part by the NSF under Grants No. PHY89-04035 and DMR92-25027.

APPENDIX

The explicit formulas for the electronic self-energy through fourth order and for the irreducible vertex function in the CDW channel are given here. The diagrammatic expansion for the self-energy is shown in Fig. 8. The first two lines include the contributions from the FLEX approximation (truncated at fourth order) while the last two lines include the extra fourth-order contributions. The self-energy is then expanded as

$$\Sigma(i\omega_n) \equiv \Sigma_n = \Sigma_n^{\rm FLEX}(4) + \Sigma_n'(4) \ , \tag{A1}$$

with $\Sigma_n^{\rm FLEX}(4)$ the contributions to the self-energy included in the FLEX approximation[15] (but truncated to fourth order) and $\Sigma_n'(4)$ the additional contributions to fourth order. The truncated FLEX contributions are[15]

$$\Sigma_n^{\rm FLEX}(4) = TU\sum_l G_{n-l}[U\chi_l^{ph} + U^2\chi_l^{ph2} + 2U^3\chi_l^{ph3}] + TU\sum_l G_{-n-1+l}[U^2\chi_l^{pp2} - U^3\chi_l^{pp3}] \ , \tag{A2}$$

through fourth order. Here the bare particle-hole and particle-particle susceptibilities are

$$\chi^{ph}(i\nu_l) = \chi_l^{ph} = -T\sum_r G_r G_{r+l} \ , \qquad \chi^{pp}(i\nu_l) = \chi_l^{pp} = T\sum_r G_r G_{-r-1+l} \ . \tag{A3}$$

The additional fourth-order contributions to the self-energy are

$$\begin{aligned}\Sigma_n'(4) = {} & T^2U^4\sum_{ll'} G_{n-l}G_{n-l+l'}G_{n+l'}\chi_l^{ph}\chi_{l'}^{ph} + 2T^2U^4\sum_{ll'} G_{-n-1+l}G_{-n-1+l-l'}G_{n+l'}\chi_l^{pp}\chi_{2n+1-l+l'}^{ph} \\ & -T^3U^4\sum_{rll'} G_{n-l}G_rG_{r+l}G_{r+l+l'}G_{r+l'}\chi_{l'}^{ph} - T^3U^4\sum_{rll'} G_{n-l}G_{n-l'}G_rG_{r-l+l'}G_{r+l'}\chi_{n+r+1-l}^{pp} \\ & +T^3U^4\sum_{rll'} G_{n-l}G_{n-l'}G_rG_{r+l}G_{r+l'}\chi_{n-r-l-l'}^{ph} \ .\end{aligned} \tag{A4}$$

At half filling the Green's functions are purely imaginary and satisfy $G_{-n-1} = -G_n$. Therefore, the particle-hole and particle-particle susceptibilities in Eq. (A3) are equal. It is easy to show that the two third-order contributions to $\Sigma^{\rm FLEX}(4)$ vanish in this case, and that the three fourth-order contributions are equal. Similarly, the three terms that involve a double summation in Eq. (A4) are equal, and so are the three triple-summation terms as shown by Yamada.[39]

The irreducible vertex function in the CDW channel can also be determined. The vertex function is broken up into its FLEX contributions and its additional fourth-order contributions

$$\Gamma_{mn}^{\rm CDW} = \Gamma_{mn}^{\rm FLEX}(4) + \Gamma_{mn}'(4) \ . \tag{A5}$$

The FLEX contributions through fourth order are[15]

$$\begin{aligned}\Gamma_{mn}^{\rm FLEX}(4) = {} & U + U^2\chi_{m-n}^{ph}[2 + U\chi_{m-n}^{ph} + 2U^2\chi_{m-n}^{ph2}] - U^2\chi_{m+n+1}^{pp}[1 - U\chi_{m+n+1}^{pp} + U^2\chi_{m+n+1}^{pp2}] \\ & -2TU^2\sum_r G_rG_{n-m+r}[U\chi_{m-r}^{ph} + 3U^2\chi_{m-r}^{ph2}] - 2TU^2\sum_r G_rG_{m+n-r}[U\chi_{m-r}^{ph} + 3U^2\chi_{m-r}^{ph2}] \\ & -2TU^2\sum_r G_rG_{m-n+r}[-2U\chi_{m+r+1}^{pp} + 3U^2\chi_{m+r+1}^{pp2}] \ ,\end{aligned} \tag{A6}$$

and the additional fourth-order contributions are

$$\begin{aligned}\Gamma_{mn}'(4) = {} & 2TU^4\sum_r G_rG_{n-m+r}[\chi_{m-r}^{ph}\chi_{n+r+1}^{pp} + \chi_{m-n}^{ph}\chi_{m-r}^{ph} + \chi_{m-n}^{ph}\chi_{n+r+1}^{pp}] \\ & +TU^4\sum_r G_rG_{m+n-r}[2\chi_{m-r}^{ph}\chi_{m+n+1}^{pp} + \chi_{m-r}^{ph}\chi_{n-r}^{ph}] \\ & +4T^2U^4\sum_{rs} G_rG_sG_{n-r+s}G_{n-m+s}[\chi_{m-r}^{ph} + \chi_{n-r}^{ph}] \\ & -2T^2U^4\sum_{rs} G_rG_sG_{m+n-s}[G_{n+r-s}\chi_{m-r}^{ph} + G_{m+r-s}\chi_{n-r}^{ph}] \\ & -2T^2U^4\sum_{rs} G_rG_sG_{-m+r+s}G_{n-m+s}[\chi_{m-r}^{ph} + \chi_{n-r}^{ph}] \\ & -T^2U^4\sum_{rs} G_rG_s[G_{n-m+r}G_{n-m+s} - G_{m+n-r}G_{m+n-s}]\chi_{r-s}^{ph} \\ & -2T^2U^4\sum_{rs} G_rG_sG_{m+r-s}G_{n+r-s}[\chi_{m+r+1}^{pp} + \chi_{n+r+1}^{pp}] - T^2U^4\sum_{rs} G_rG_sG_{n-m+r}G_{m-n+s}\chi_{r+s+1}^{pp} \\ & -2T^2U^4\sum_{rs} G_rG_s[G_{m+r-s}G_{n-r+s}\chi_{m+r+1}^{pp} + G_{n+r-s}G_{m-r+s}\chi_{n+r+1}^{pp}] \\ & -4T^3U^4\sum_{rst} G_sG_t\mathrm{Re}[G_rG_{r+s-t}G_{-m+r+s}G_{n+r-t}] \\ & +T^3U^4\sum_{rst} G_rG_sG_tG_{r+s-t}G_{n+s-t}[G_{m-r+t} + G_{m+r-t}] \ .\end{aligned} \tag{A7}$$

Note that the simplified FLEX* approximation does not include any of the terms that involve explicit summations over Matsubara frequency [the second and third lines in Eq. (A6)].

By making the transformations $t \to r + s - t$, $r \to s$, and $s \to r$ in the triple-summation terms in Eq. (A7) and using the symmetry at half filling $G_{-n-1} = -G_n$, one can demonstrate that the triple-summation terms are *odd* under $n \to -n-1$, and do not contribute to the eigenvalue of the scattering matrix if the eigenvector is even under $n \to -n-1$. Therefore, the triple-summation terms in Eq. (A7) may be neglected (this result has been explicitly tested by calculating the eigenvalue of the scattering matrix with and without the triple-summation terms and there was no effect on the eigenvalue at half filling).

[1] *Superconductivity*, edited by R. Parks (Marcel Dekker, Inc., New York, 1969).
[2] P. B. Allen and R. C. Dynes, Phys. Rev. B **12**, 905 (1975); P. B. Allen and B. Mitrović, Solid State Phys. **37**, 1 (1982); J. P. Carbotte, Rev. Mod. Phys. **62**, 1027 (1990); H.-S. Wu, Z.-Y Weng, G. Ji, and Z.-F. Zhou, J. Phys. Chem. Solids **48**, 395 (1987).
[3] A. B. Migdal, Zh. Eksp. Teor. Fiz. **34**, 1438 (1958) [Sov. Phys. JETP **7**, 999 (1958)].
[4] G. M. Eliashberg, Zh. Eksp. Teor. Fiz. **38**, 966 (1960) [Sov. Phys. JETP **11**, 696 (1960)].
[5] R. J. Cava, B. Batlogg, J. J. Krajewski, R. Farrow, L. W. Rupp, Jr., A. E. White, K. Short, W. F. Peck, and T. Kometani, Nature **322**, 814 (1988).
[6] P. Vashishta, R. K. Kalia, M. H. Degani, D. L. Price, J. D. Jorgensen, D. G. Hinks, B. Dabrowski, A. W. Mitchell, D. R. Richards, and Y. Zheng, Phys. Rev. Lett. **62**, 2628 (1989).
[7] L. F. Mattheiss and D. R. Hamann, Phys. Rev. Lett. **60**, 2681 (1988).
[8] M. Schluter, M. Lannoo, M. Needels, G. A. Baraff, and D. Tománek, Phys. Rev. Lett. **68**, 526 (1992).
[9] S. Saito and A. Oshiyama, Phys. Rev. B **44**, 11 536 (1991).
[10] M. Grabowski and L. J. Sham, Phys. Rev. B **29**, 6132 (1984).
[11] J. Cai, X. L. Lei, and L. M. Xie, Phys. Rev. B **39**, 11 618 (1989).
[12] J. K. Freericks and D. J. Scalapino, Phys. Rev. B **49**, 6368 (1994).
[13] T. Holstein, Ann. Phys. (N.Y.) **8**, 325 (1959).
[14] J. Hubbard, Proc. R. Soc. London Ser. A **276**, 238 (1963).
[15] G. Baym and L. P. Kadanoff, Phys. Rev. **124**, 287 (1961); G. Baym, *ibid.* **127**, 1391 (1962); N. E. Bickers and D. J. Scalapino, Ann. Phys. (N.Y.) **193**, 206 (1989); N. E. Bickers and S. R. White, Phys. Rev. B **43**, 8044 (1991).
[16] P. G. J. van Dongen, Phys. Rev. Lett. **67**, 757 (1991); (unpublished).
[17] A. Martín-Rodero and F. Flores, Phys. Rev. B **45**, 13 008 (1992).
[18] P. Nozières and S. Schmitt-Rink, J. Low Temp. Phys. **59**, 195 (1985).
[19] S. Robaszkiewicz, R. Micnas, and K. A. Chao, Phys. Rev. B **23**, 1447 (1981); A. S. Alexandrov, J. Ranninger, and S. Robaszkiewicz, *ibid.* **33**, 4526 (1986); R. Micnas, J. Ranninger, and S. Robaszkiewicz, Rev. Mod. Phys. **62**, 113 (1990).
[20] W. Metzner and D. Vollhardt, Phys. Rev. Lett. **62**, 324 (1989).
[21] J. K. Freericks, M. Jarrell, and D. J. Scalapino, Phys. Rev. B **48**, 6302 (1993); Europhys. Lett. **25**, 37 (1994).
[22] M. Jarrell, Phys. Rev. Lett. **69**, 168 (1992); M. Jarrell and Th. Pruschke, Z. Phys. B **90**, 187 (1993); Th. Pruschke, D. L. Cox, and M. Jarrell, Phys. Rev. B **47**, 3553 (1993).
[23] M. J. Rozenberg, X. Y. Zhang, and G. Kotliar, Phys. Rev. Lett. **69**, 1236 (1992).
[24] A. Georges and W. Krauth, Phys. Rev. Lett. **69**, 1240 (1992); Phys. Rev. B **48**, 7167 (1993).
[25] J. E. Hirsch and R. M. Fye, Phys. Rev. Lett. **56**, 2521 (1986).
[26] H. Schweitzer and G. Czycholl, Z. Phys. B **77**, 327 (1990).
[27] W. Metzner, Phys. Rev. B **43**, 8549 (1991).
[28] U. Brandt and C. Mielsch, Z. Phys. B **75**, 365 (1989).
[29] F. J. Ohkawa, Phys. Rev. B **44**, 6812 (1991); Prog. Theor. Phys. Suppl. **106**, 95 (1991).
[30] A. Georges and G. Kotliar, Phys. Rev. B **45**, 6479 (1992).
[31] V. Zlatić and B. Horvatić, Solid State Commun. **75**, 263 (1990).
[32] E. Müller-Hartmann, Z. Phys. B **74**, 507 (1989); **76**, 211 (1989).
[33] S. Ciuchi, F. de Pasquale, C. Masciovecchio, and D. Feinberg, Europhys. Lett. **24**, 575 (1993).
[34] F. Marsiglio, Phys. Rev. B **42**, 2416 (1990).
[35] C. S. Owen and D. J. Scalapino, Physica **55**, 691 (1971).
[36] J. Bardeen, L. N. Cooper, and J. R. Schrieffer, Phys. Rev. **108**, 1175 (1957).
[37] D. S. Hirashima, Phys. Rev. B **47**, 15 428 (1993).
[38] B. Menge and E. Müller-Hartmann, Z. Phys. B **82**, 237 (1991).
[39] K. Yamada, Prog. Theor. Phys. **55**, 1345 (1976).
[40] L. G. Aslamazov and A. I. Larkin, Fiz. Tverd. Tela (Leningrad) **10**, 1104 (1968) [Sov. Phys. Solid State **10**, 875 (1968)].
[41] J. A. White, Phys. Rev. B **45**, 1100 (1992).